J. Fluid Mech. (1986), *vol.* 169, *pp.* 307–322
Printed in Great Britain

Thick $E^{\frac{1}{4}}$ Stewartson layers in a rapidly rotating gas

By LENNART S. HULTGREN

Department of Mechanical and Aerospace Engineering, Illinois Institute of Technology, Chicago, IL 60616

AND FRITZ H. BARK

Department of Mechanics, Royal Institute of Technology, S-100 44 Stockholm, Sweden

(Received 17 October 1985)

The effects of circumferential curvature and strong density variation on $E^{\frac{1}{4}}$ Stewartson layers are investigated. The solution of the third-order ordinary differential equation found to govern the flow is obtained by numerical integration for layers extending in the positive radial direction and in terms of a Frobenius-series solution for layers extending in the opposite direction. Due to the variation of the basic density field, the $E^{\frac{1}{4}}$ layer is compressed in the positive radial direction. $E^{\frac{1}{4}}$ layers extending in the negative radial direction are likely to extend fully to the axis of symmetry because of the density variation and, consequently, a distinction in terms of a geostrophic flow and an $E^{\frac{1}{4}}$ layer flow cannot be made. Curvature effects are found to play a significant role in this case. A simple case of driving by a differential rotation of part of the horizontal boundaries is examined.

1. Introduction

The dynamics of contained rapidly rotating gases has received considerable attention in connection with the interest in Uranium hexafluoride (UF_6) gas centrifuges during the last decade. These centrifuges usually operate with a peripheral Mach number between one and ten. It is well known (cf. Howard 1970; Sakurai & Matsuda 1974; Olander 1978) that a variety of boundary-layer and shear-layer phenomena arise in rapidly rotating gas flows, and that the flow may often be controlled by these boundary layers. For the case where the ratio of the scale height of the basic density field and the boundary-layer thickness is infinitely large, Sakurai & Matsuda (1974) found that the compressible Stewartson $E^{\frac{1}{3}}$ layer is quite similar to the corresponding layer for a homogeneous fluid. The effects of a weak variation of the density field of the rigidly rotating gas across the Stewartson layer have been investigated by Mikami (1973), Nakayama & Usui (1974), Durivault *et al.* (1976), Durivault & Louvet (1976), Louvet & Durivault (1976), and Bark & Bark (1976) for the $E^{\frac{1}{3}}$ layer and by Nakayama & Usui (1974) and Bark & Bark (1976) for the $E^{\frac{1}{4}}$ layer. These approximate solutions are valid near the periphery of gas centrifuges, where the Stewartson layers are thin, and thus the variation of the density field across such layers is small.

In most of the centrifuge, the situation is different however. Owing to the rapid rotation, the density is in practice usually very small apart from the immediate neighbourhood of the periphery. This has some interesting consequences for the structure of the boundary layers. Because the gas centrifuges, in general, are slender the local Ekman number is usually sufficiently small everywhere for Ekman-layer

flow to occur at the top and bottom boundaries, but it can be shown that Stewartson layers outside the immediate neighbourhood of the periphery do often have a radial lengthscale of the same order of magnitude as the radial dimension of the container. These layers may be characterized as thick, and they are influenced by both a strong density variation across the layer and curvature effects. Bark & Meijer (1982) have investigated the structure of such a thick $E^{\frac{1}{3}}$ Stewartson layer. They found that the layer is compressed in the positive radial direction, but is expanded in the opposite direction. If an inner cylinder is present, a weak geostrophic flow was shown to appear in the outer parts of the container for sufficiently large Mach numbers.

It is the purpose of the present investigation to analyse the structure of thick $E^{\frac{1}{4}}$ Stewartson layers. The heavy-gas limit is discussed in Appendix B.

2. Formulation

Consider an ideal, viscous and heat conducting gas of constant temperature T^*_∞. The gas is contained in a straight cylindrical or annular vessel with flat top and bottom caps. The container walls are assumed to be perfectly thermally conducting. For containers with thermally insulating walls, the boundary-layer structure will be different from the present one (Bark & Hultgren 1979). The container is rotating around its axis of symmetry with the constant angular velocity Ω. The rate of rotation is taken to be very large in the sense that effects of gravity are ignored. A cylindrical coordinate system (r, ϕ, z) is to be used with the z-axis coinciding with the axis of rotation. The radial and axial coordinates are non-dimensionalized with half the container height H. The top and bottom are thus taken to be at $z = \pm 1$.

For a rigidly rotating isothermal gas, the non-dimensional density and pressure fields are given by

$$\rho_0(r) = \exp\left\{\tfrac{1}{2}\gamma M^2\left(\left(\frac{r}{r_0}\right)^2 - 1\right)\right\}, \tag{2.1}$$

$$p_0(r) = \frac{r_0^2}{\gamma M^2}\rho_0(r), \tag{2.2}$$

where r_0 is a non-dimensional reference radius, $\gamma = c_p/c_v$ is the ratio of specific heats at constant pressure and volume, and

$$M = \frac{r_0 H\Omega}{(\gamma R T^*_\infty)^{\frac{1}{2}}} \tag{2.3}$$

is a local Mach number at the radial location r_0. R is the gas constant. The reference density ρ^*_∞ is that at the reference radius, and the pressure scale is $\rho^*_\infty(H\Omega)^2$.

Small steady axisymmetric perturbations on the state of isothermal rigid-body rotation will be considered. The deviation flow field is assumed to be caused by differential rotation or axisymmetric heating of both of the horizontal boundaries. The driving is assumed to be symmetric with respect to $z = 0$. A Rossby number can be defined as

$$\epsilon = \frac{\Delta\Omega}{\Omega}, \tag{2.4}$$

where $\Delta\Omega$ is a characteristic differential angular velocity of the boundaries. If the perturbation motion is due to differential heating, a Rossby number can be defined in an analogous manner. The Rossby number is assumed to be very small so that

linear theory can be used. The dependent variables of the perturbation flow field are scaled as

$$\boldsymbol{u}^* = \epsilon H\Omega \boldsymbol{u}, \quad p^* = \epsilon \rho_\infty^* (H\Omega)^2 p, \tag{2.5a, b}$$

$$\rho^* = \epsilon \rho_\infty^* \rho, \quad T^* = \epsilon T_\infty^* T, \tag{2.5c, d}$$

where an asterisk denotes dimensional variables, $\boldsymbol{u} = (u, v, w)$ is the velocity, p is the pressure, ρ is the density, and T is the temperature.

Using (2.5), the following linearized equations for the perturbation motion can be derived: the equation of continuity

$$\frac{1}{r}\frac{\partial}{\partial r}(r\rho_0 u) + \rho_0 \frac{\partial w}{\partial z} = 0; \tag{2.6}$$

the equations of conservation of momentum

$$-2\rho_0 v - \rho r = -\frac{\partial p}{\partial r} + E\left[\left(\nabla^2 - \frac{1}{r^2}\right)u + (\tfrac{1}{3}+\zeta)\frac{\partial}{\partial r}(\nabla\cdot\boldsymbol{u})\right], \tag{2.7a}$$

$$2\rho_0 u = E\left(\nabla^2 - \frac{1}{r^2}\right)v, \tag{2.7b}$$

$$0 = -\frac{\partial p}{\partial z} + E\left[\nabla^2 w + (\tfrac{1}{3}+\zeta)\frac{\partial}{\partial z}(\nabla\cdot\boldsymbol{u})\right]; \tag{2.7c}$$

the energy equation

$$-4\alpha^2 r\rho_0 u = E\nabla^2 T; \tag{2.8}$$

the equation of state

$$p = \frac{r_0^2}{\gamma M^2}(\rho + \rho_0 T); \tag{2.9}$$

where

$$E = \frac{\mu}{\rho_\infty^* H^2 \Omega}, \tag{2.10a}$$

is the local Ekman number at the reference radius r_0,

$$\alpha^2 = \frac{\sigma(\gamma-1)M^2}{4r_0^2}, \tag{2.10b}$$

and ζ is the ratio of the bulk and dynamic shear viscosities. μ is the dynamic shear viscosity,

$$\sigma = \frac{\mu c_p}{k}, \tag{2.10c}$$

is the Prandtl number, and k is the thermal conductivity. μ, ζ, k, c_p and γ are assumed to be constants. The parameters σ, ζ and γ are assumed to be of order unity, whereas the Ekman number E is taken to be vanishingly small.

The system of equations (2.6)–(2.9) are to be solved subject to the boundary conditions

$$\boldsymbol{u}(r, \pm 1) = v_{\mathrm{B}}(r)\,\boldsymbol{e}_\phi, \quad r_{\mathrm{i}} \leqslant r \leqslant r_{\mathrm{p}}, \tag{2.11a}$$

$$\boldsymbol{u}(r_{\mathrm{i}}, z) = \boldsymbol{u}(r_{\mathrm{p}}, z) = 0, \quad -1 < z < 1, \tag{2.11b}$$

$$T(r, \pm 1) = T_{\mathrm{B}}(r), \quad r_{\mathrm{i}} \leqslant r \leqslant r_{\mathrm{p}}, \tag{2.11c}$$

$$T(r_{\mathrm{i}}, z) = T(r_{\mathrm{p}}, z) = 0, \quad -1 < z < 1, \tag{2.11d}$$

where v_{B} and T_{B} are the prescribed azimuthal velocity and temperature distributions of the horizontal boundaries, $\boldsymbol{e}_\phi$ is the unit vector in the azimuthal direction and r_{i} and r_{p} are the inner and outer radii of the annulus respectively. If the container is

a cylinder r_i is equal to zero, and the boundary conditions at that radius are replaced by the condition that all physical quantities be bounded on the axis of symmetry.

The motion in the interior is described by the limiting solution to (2.6)–(2.9) when the Ekman number tends to zero. For the case of symmetric forcing, this geostrophic flow has been discussed by Hashimoto (1977) and Bark & Hultgren (1979). Therefore, only the essential features of this flow need be described here. In contrast to a homogeneous fluid, the geostrophic azimuthal velocity component is not independent of the axial coordinate. Also, the lowest-order Ekman layers disappear if the forcing is symmetric, and, in that case, the geostrophic flow field must itself satisfy the no-slip and thermal boundary conditions at the horizontal walls. Vertical $E^{\frac{1}{4}}$ and $E^{\frac{1}{3}}$ Stewartson layers, in general, appear at vertical boundaries and at radii where there are discontinuities in the prescribed driving at $z = \pm 1$. The vertical boundary layers have been discussed by, among others, Bark & Bark (1976) for the case when the boundary-layer thickness is small but finite compared with the basic density scale height. These investigators presented an exact solution for the $E^{\frac{1}{4}}$ layer, a numerical solution for the $E^{\frac{1}{3}}$ layer, as well as uniformly valid asymptotic solutions for both layers. The internal flow in gas centrifuges has also been analysed using the Onsager's pancake approximation by Wood & Morton (1980) and, with curvature effects incorporated by Wood, Jordan & Gunzburger (1984).

Because of the rapid rotation of practical gas centrifuges, the local Ekman number can vary by several orders of magnitude across the radial extent of the container. As a consequence, Stewartson layers in the centre region of the container are much thicker than the ones at the periphery. Also, UF_6 centrifuges are usually very slender because their separation efficiency increases with the height of the device. Thus, a Stewartson layer in the vicinity of the axis of rotation is not only affected by the strong density variation across the layer, but also by its circumferential curvature.

In order to account for these properties of the flow in a thick $E^{\frac{1}{4}}$ layer, a limit process similar to the one used by Bark & Meijer (1982) for a thick $E^{\frac{1}{3}}$ layer will be used, namely

$$E \to 0, \quad r_0 = O(E^{\frac{1}{4}}), \quad M = O(1), \quad \text{fixed}. \tag{2.12a, b, c}$$

Equation (2.12*b*) means that the layer is in the neighbourhood of the axis of symmetry; (2.12*c*) implies that the scale height of the basic density field is $O(E^{\frac{1}{4}})$ at the reference radius. In view of (2.12*b*), a stretched coordinate is suitably defined as

$$\eta = \frac{r}{E^{\frac{1}{4}}}. \tag{2.13}$$

The basic density field can be written in terms of the stretched coordinate as

$$\rho_0(\eta) = \exp\left(\frac{\gamma M^2}{2\eta_0^2}(\eta^2 - \eta_0^2)\right), \tag{2.14a}$$

where

$$\eta_0 = \frac{r_0}{E^{\frac{1}{4}}} = O(1). \tag{2.14b}$$

An order-of-magnitude analysis shows that a meaningful perturbation problem can be constructed if

$$u = O(E^{\frac{3}{4}}), \quad v = O(E^{\frac{1}{4}}), \quad w = O(E^{\frac{1}{2}}), \tag{2.15a–c}$$

$$p = O(E^{\frac{1}{2}}), \quad \rho = O(1), \quad T = O(1). \tag{2.15d–f}$$

Using (2.6)–(2.9) and (2.14) and rescaling the dependent variables as indicated by (2.15), one finds the following leading-order equations:

$$\frac{1}{\eta}\frac{\partial}{\partial\eta}(\eta\rho_0 u)+\rho_0\frac{\partial w}{\partial z}=0, \tag{2.16}$$

$$2\rho_0 v+\rho\eta=\frac{\partial p}{\partial\eta}, \tag{2.17a}$$

$$2\rho_0 u=\left(\frac{1}{\eta}\frac{\partial}{\partial\eta}\left(\eta\frac{\partial}{\partial\eta}\right)-\frac{1}{\eta^2}\right)v, \tag{2.17b}$$

$$\frac{\partial p}{\partial z}=0, \tag{2.17c}$$

$$-4\kappa^2\rho_0\eta u=\frac{1}{\eta}\frac{\partial}{\partial\eta}\left(\eta\frac{\partial T}{\partial\eta}\right), \tag{2.18}$$

$$p=\frac{\eta_0^2}{\gamma M^2}(\rho+\rho_0 T), \tag{2.19}$$

where

$$\kappa^2=\alpha^2E^{\frac{1}{2}}=\frac{\sigma(\gamma-1)M^2}{4\eta_0^2}=O(1). \tag{2.20}$$

From (2.16) to (2.19) it follows that all quantities are independent of the axial coordinate except for w, which is linear in z. Combination of (2.17b) and (2.18), followed by integration once, yields

$$\frac{\mathrm{d}T}{\mathrm{d}\eta}+2\kappa^2\eta^2\frac{\mathrm{d}}{\mathrm{d}\eta}\left(\frac{v}{\eta}\right)=\frac{2c_1}{\eta}, \tag{2.21}$$

where c_1 is a constant of integration. From (2.14a), (2.17a) and (2.19) one can derive the following equation:

$$v=\tfrac{1}{2}\eta T+\frac{1}{2}\frac{\mathrm{d}q}{\mathrm{d}\eta}, \tag{2.22a}$$

where

$$q=\frac{p}{\rho_0}. \tag{2.22b}$$

At the horizontal boundaries, two corner regions of sizes $E^{\frac{1}{2}}\times E^{\frac{1}{4}}$ and $E^{\frac{1}{4}}\times E^{\frac{1}{4}}$ respectively, are needed in order to fulfil the no-slip and thermal boundary conditions. The analysis of the corner regions is straightforward and similar to the one given in Hultgren, Meijer & Bark (1981). One finds the following Ekman suction formula:

$$w(\eta,\pm1)=\mp\frac{1}{2\rho_0\eta}\frac{\mathrm{d}}{\mathrm{d}\eta}\{\eta\rho_0^{\frac{1}{2}}(1+\kappa^2\eta^2)^{-\frac{3}{4}}(v-v_{\mathrm{B}}+\tfrac{1}{2}\eta(T-T_{\mathrm{B}}))\}. \tag{2.23}$$

The equations (2.16), (2.17b), (2.22a) and (2.23) lead to

$$\frac{\mathrm{d}q}{\mathrm{d}\eta}=2\rho_0^{-\frac{1}{2}}(1+\kappa^2\eta^2)^{\frac{3}{4}}\frac{1}{\eta^2}\frac{\mathrm{d}}{\mathrm{d}\eta}\left(\eta^3\frac{\mathrm{d}}{\mathrm{d}\eta}\left(\frac{v}{\eta}\right)\right)+2(v_{\mathrm{B}}-\tfrac{1}{2}\eta T_{\mathrm{B}}). \tag{2.24}$$

Finally, combination of (2.21), (2.22a) and (2.24) leads to a non-homogeneous third-order ordinary differential equation governing the azimuthal velocity component. By inspection, one finds that a homogeneous solution to this equation is

given by $v = \eta$. The method of reduction of order then yields the following second-order differential equation:

$$\frac{\mathrm{d}}{\mathrm{d}\eta}\left(\frac{(1+\kappa^2\eta^2)^{\frac{1}{2}}}{\eta^3\rho_0^{\frac{1}{2}}}\frac{\mathrm{d}}{\mathrm{d}\eta}(\eta^3 g)\right)-(1+\kappa^2\eta^2)\,g = -\frac{\mathrm{d}}{\mathrm{d}\eta}\left(\frac{1}{\eta}(v_{\mathrm{B}}-\tfrac{1}{2}\eta T_{\mathrm{B}})\right)-\frac{c_1}{\eta}. \tag{2.25a}$$

where

$$g = f' \tag{2.25b}$$

and the azimuthal velocity is given by

$$v = \eta f. \tag{2.25c}$$

The quantity $\mathrm{d}q/\mathrm{d}\eta$ can be computed from g using (2.24). When this quantity and the azimuthal velocity have been determined, the temperature field can be computed through (2.22*a*). As an alternative, the temperature field can be constructed from g by integrating (2.21). The solution of (2.21) and (2.25) for the centre region ($0 \leqslant \eta < \eta_0$) and the outer region ($\eta > \eta_0$) will respectively be described in the following two sections.

3. The centre region

For the case when there is a discontinuity in the external driving, but no inner solid boundary, at the radius r_0, the $E^{\frac{1}{4}}$ layer extending in the negative radial direction is likely to extend all the way to the axis of symmetry. By considering the behaviour for small η, inspection of (2.22*a*) and (2.21) gives

$$c_1 = 0 \tag{3.1}$$

in order for the physical variables to remain finite at the origin. A Frobenius-series solution for the dependent variable g can be constructed in a straightforward manner and the velocity and temperature fields can be constructed therefrom. The details of this procedure are given in Appendix A. One finds

$$v = (\omega - \tfrac{1}{2}(\theta - T_0))\,\eta + Bv_{\mathrm{C}}(\eta) + v_{\mathrm{P}}(\eta), \tag{3.2}$$

$$T = T_0 + BT_{\mathrm{C}}(\eta) + T_{\mathrm{P}}(\eta), \tag{3.3}$$

where ω and θ are given by (A 8); B and T_0 are constants of integration; v_{C} and T_{C} are the homogeneous solutions; and v_{P} and T_{P} are the particular solutions corresponding to the non-homogeneous term in (2.25*a*). In the limit of the Mach number tending to zero, v_{C} and T_{C} become $I_1(\eta)$ and zero respectively, where I_1 is the modified Bessel function, see Appendix B.

The Frobenius-series solutions were used to calculate the dependent variables v_{C} and T_{C} taking the physical parameters to be those of UF_6 at room temperature, i.e. $\gamma = 1.067$ and $\sigma = 0.95$. Figure 1 shows the azimuthal velocity and the temperature for Mach numbers equal to 0, 1, 2 and 5 for the case when the radius $\eta_0 = 1$. Figure 2 shows the corresponding results for $\eta_0 = 10$. As the Mach number increases, the swirl velocity approaches rigid-body rotation over a large portion of the interval. The reason for this can be deduced from (2.25*a*): as the density distribution becomes vanishingly small, g must also vanish in order to remain finite at the origin and, hence, the azimuthal velocity approaches rigid-body rotation. From (2.21) it then follows that the temperature must approach a constant in most of the centre region. That the latter is indeed the case can be seen in figures 1(*b*) and 2(*b*).

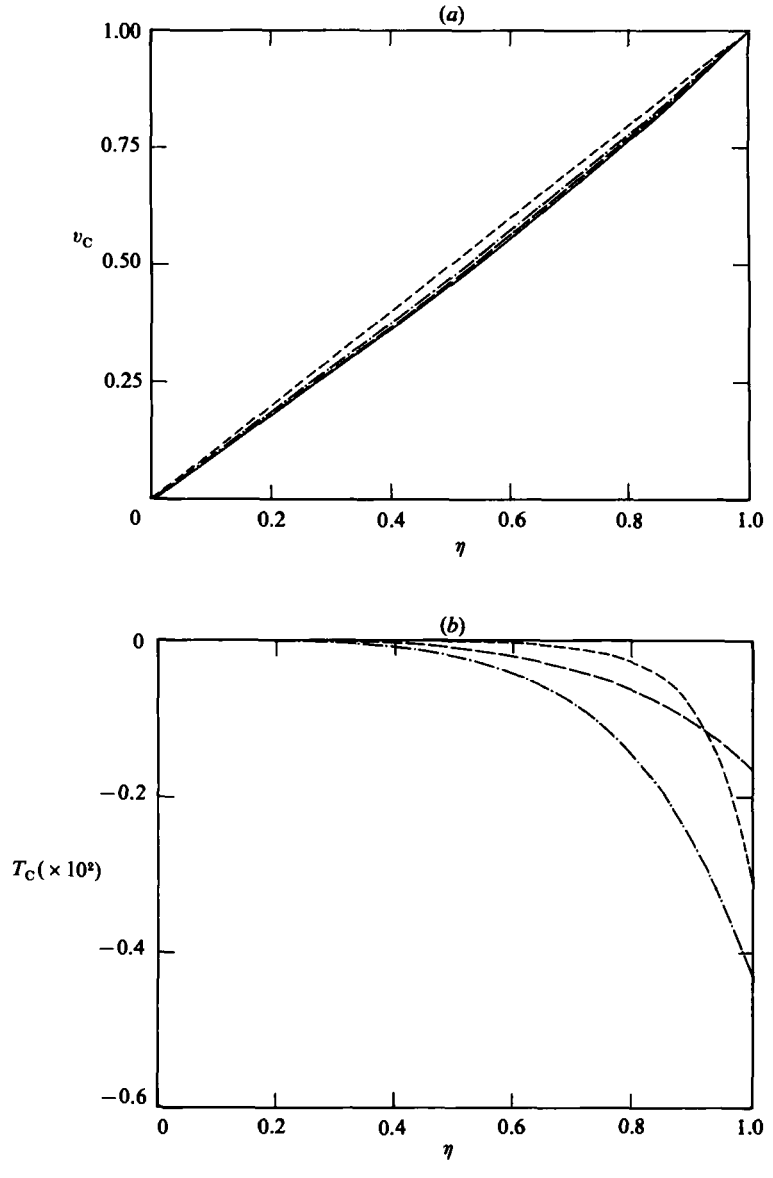

FIGURE 1. Centre-region solution, $\eta_0 = 1$: ——, $M = 0$; – – –, 1; – · –, 2; ------, 5. (*a*) azimuthal velocity. (*b*) temperature.

4. The outer region

For the flow region extending in the positive radial direction, the particular solution to (2.25) can be interpreted as the geostrophic flow, and the homogeneous solutions are associated with flow in the Stewartson layers. For large values of ρ_0, i.e. as $\eta \to +\infty$, the following approximations of the solutions to (2.26*a*) can be constructed:

$$g_I \approx \frac{c_1}{\eta(1+\kappa^2\eta^2)} + \frac{1}{1+\kappa^2\eta^2}\frac{d}{d\eta}\left(\frac{1}{\eta}(v_B - \tfrac{1}{2}\eta T_B)\right), \tag{4.1}$$

$$g_\pm \approx \eta^{-\frac{3}{2}}(1+\kappa^2\eta^2)^{-\frac{7}{16}}\rho_0^{-\frac{1}{8}}\, e^{\mp\eta_+}, \tag{4.2a}$$

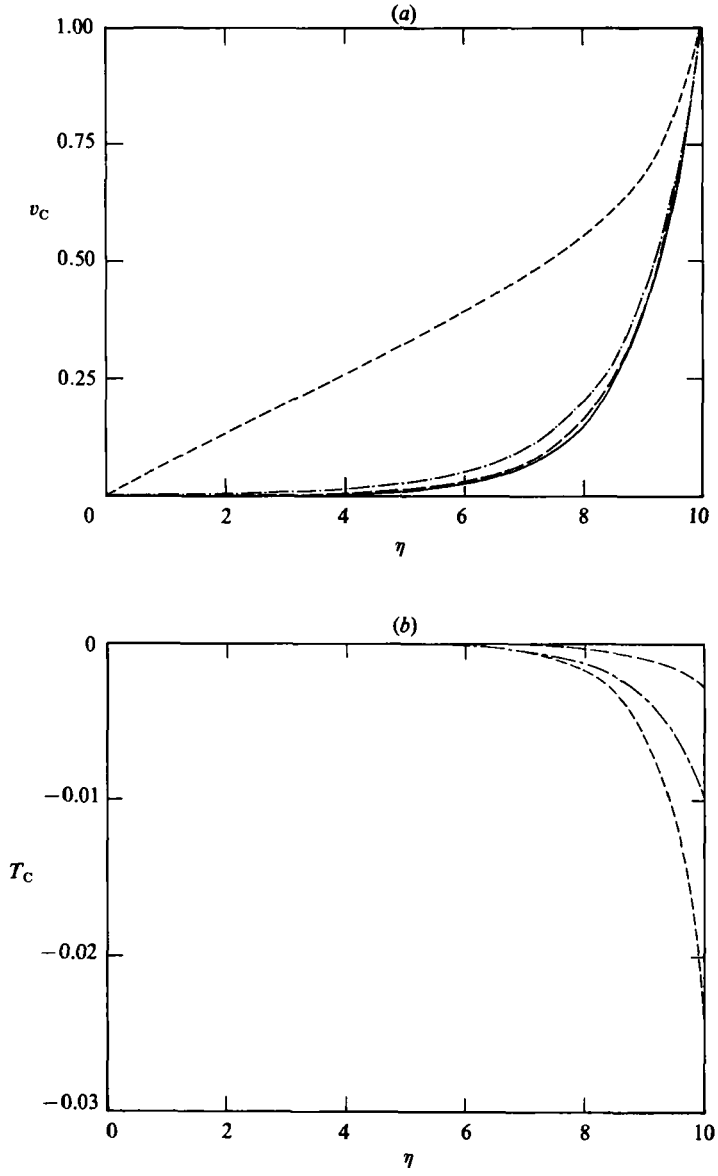

FIGURE 2. As figure 1 except $\eta_0 = 10$.

where g_I is the particular solution, $g_\pm$ are the homogeneous solutions, and

$$\eta_+ = \int_{\eta_0}^{\eta} (1+\kappa^2\eta'^2)^{\frac{1}{8}}\rho_0^{\frac{1}{4}}(\eta')\,\mathrm{d}\eta' \tag{4.2b}$$

is a fast variable. As $\eta_0 \to +\infty$, the WKB-type solution (4.2) reduces to the leading-order approximation for the Stewartson layer given by Bark & Bark (1976) for the case when the density variation is weak across the layer, and the solution given by Sakurai & Matsuda (1974) when there is no density variation. Integration of (4.1) gives

$$f_I \approx c_1(\ln\eta - \tfrac{1}{2}\ln(1+\kappa^2\eta^2)) + c_2 + \int_{\eta_p}^{\eta} \frac{1}{1+\kappa^2\eta'^2}\frac{\mathrm{d}}{\mathrm{d}\eta'}\left(\frac{1}{\eta'}(v_B - \tfrac{1}{2}\eta' T_B)\right)\mathrm{d}\eta', \tag{4.3}$$

where $\eta_p = r_p/E^{\frac{1}{4}}$ and c_2 is a constant of integration. The azimuthal velocity corresponding to (4.3) is obtained through (2.25c) and the temperature is approximated by

$$T_I \approx 2f_I. \tag{4.4}$$

It is easily verified that (4.3) and (4.4) correspond to the slender-centrifuge approximation (Bark & Bark 1979) for the geostrophic flow. If, for the Stewartson layer at the periphery, the density variation is weak and the effects of curvature can be ignored, then, with the boundary conditions (2.11), this layer does not occur to leading order and the vertically averaged geostrophic azimuthal velocity and temperature fields must vanish at the solid boundary. Assuming $r_p/H = o(1)$, i.e. invoking the slender-centrifuge approximation, then leads to

$$c_2 = -c_1(\ln \eta_p - \tfrac{1}{2}\ln(1+\kappa^2\eta_p^2)). \tag{4.5}$$

The solution g_+ in (4.2) was used to give starting values to a three-step fourth-order Runge–Kutta scheme, which, in turn, provided the starting values for the numerical integration towards η_0 using a fourth-order Adams implicit method (cf. Collatz 1960, p. 126). Once the appropriate solution to (2.25a) had been obtained, it was numerically integrated once, again using a fourth-order Adams implicit method. The azimuthal velocity could then be obtained from (2.25c). The temperature field was then computed by using (2.22a) and (2.24) (with $v_B = T_B = 0$). These solutions will be referred to as v_S and T_S. In the limit of the Mach number tending to zero, v_S and T_S approach $K_1(\eta)$ and zero respectively, where K_1 is the modified Bessel function, see Appendix B.

In the numerical calculations presented here the physical parameters are the same as in the previous section, i.e. $\gamma = 1.067$ and $\sigma = 0.95$. The radius η_0 was taken to equal unity. Calculations were performed for Mach numbers equal to 0, 1, 2 and 5. The azimuthal velocity v_S and the temperature T_S are shown in figure 3. The solutions were normalized such that the azimuthal velocity equalled unity at $r = r_0$. The strong increase of the basic density field in the positive radial direction significantly reduces the boundary-layer thickness compared with the case when the basic density scale height is infinitely large in comparison with the boundary-layer scale. These results are in agreement with those of Bark & Bark (1976), who found that the boundary layer is slightly compressed when there is a weak variation of the density across the layer, and the findings by Bark & Meijer (1982) for thick $E^{\frac{1}{3}}$ Stewartson layers.

5. A simple example

As a simple illustrative example, the following form of the forcing was assumed:

$$v_B = \omega\eta, \quad 0 \leqslant \eta < \eta_0, \tag{5.1a}$$

$$v_B = 0, \quad \eta_0 < \eta \leqslant \eta_p, \tag{5.1b}$$

$$T_B = 0, \quad 0 \leqslant \eta \leqslant \eta_p. \tag{5.1c}$$

In this case, the particular solutions v_P and T_P do not appear. The conditions to be applied at $\eta = \eta_0$ are that the azimuthal velocity, the temperature and their first derivatives are continuous. The conditions on the first derivatives follow from the fact that the flow cannot sustain any shear discontinuities nor contain any heat sources. These four conditions lead to a four-by-four system of linear equations for the unknowns T_0, B, C and c_1, where C is the multiplicative constant of integration for the Stewartson layer extending in the positive radial direction (see §§3 and 4).

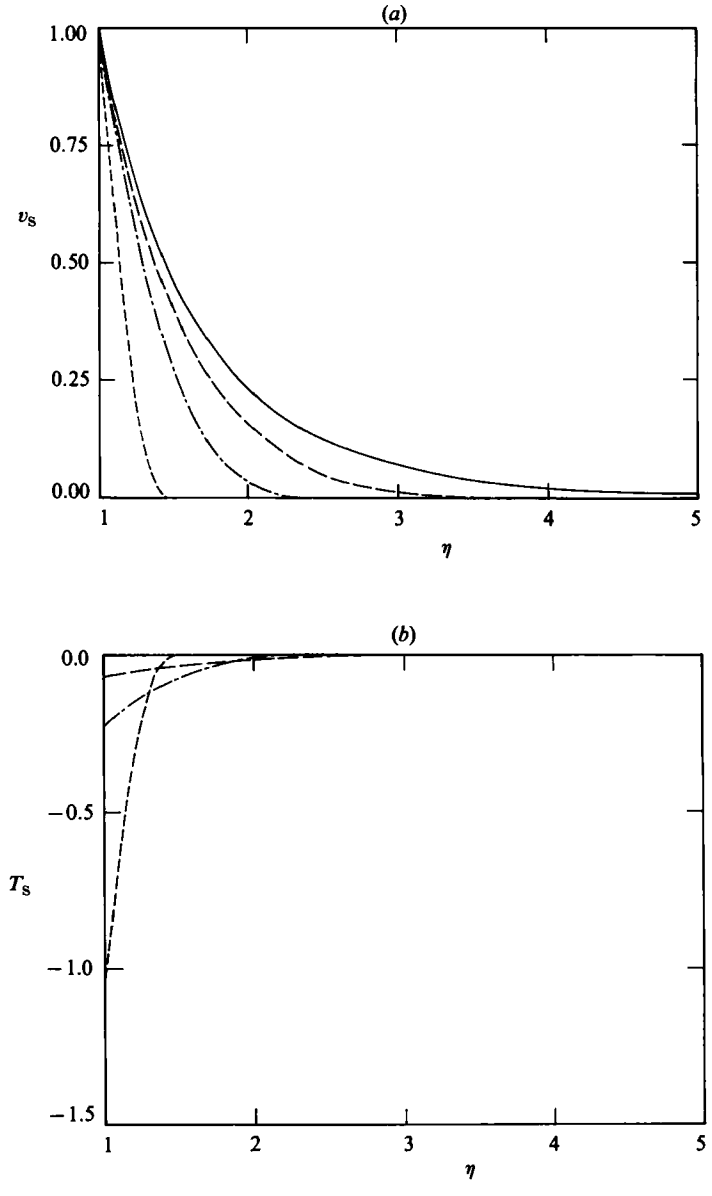

FIGURE 3. $E^{\frac{1}{4}}$ layer extending in the positive radial direction, $\eta_0 = 1$. For legend see figure 1.

The solutions v_I and T_I were obtained using (4.1), (4.3) and (4.5) to provide starting values for a numerical procedure analogous to the one utilized to obtain v_S and T_S. The system of equations was then solved using the IMSL routine LEQT2F. In all cases investigated, the constant c_1 was found to be smaller than the judged accuracy of the solution. Hence, it has been shown numerically that, in this case, a geostrophic flow does not appear in the outer region. Also, it is shown in Appendix B that c_1 equals zero in the leading-order approximation for the heavy-gas case.

Figures 4 and 5 both show the total azimuthal velocity and temperature distributions for Mach numbers equal to 0, 1, 2 and 5. The values of the physical parameters are the same as in the previous sections, i.e. those of UF_6 at room temperature, and the

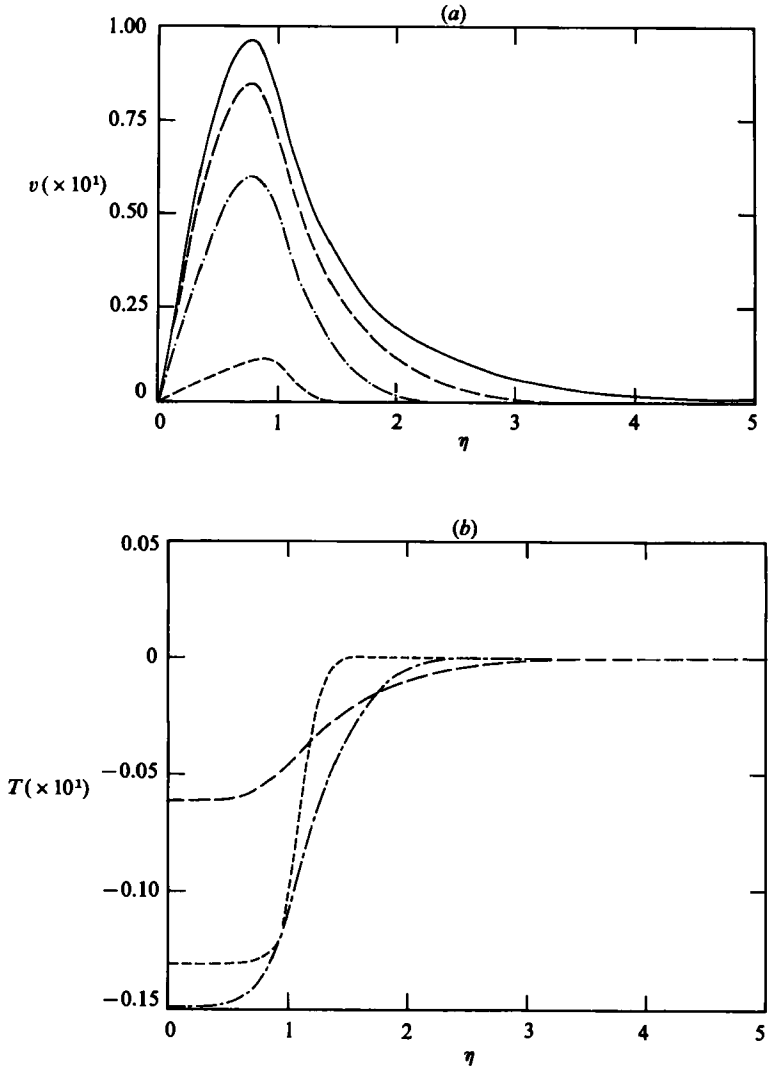

FIGURE 4. Response to differential rotation, $\eta_0 = 1$. For legend see figure 1.

radius $\eta_0 = 1$ and 10 in figures 4 and 5 respectively. (For the purpose of determining v_I and T_I, the peripheral radius η_p was taken to equal 5 and 10 for the cases corresponding to these two figures respectively.)

As can be seen in these figures, both density variation and curvature effects have a strong influence on the solution. For large values of η_0, where curvature effects are of minor importance, a geostrophic zone can be identified in the centre region. In this zone, the gas is rotating rigidly and has a constant temperature. The dependent variables undergo a rapid change at the radius where the discontinuity in the driving occurs, i.e. a vertical shear layer can be identified there. For small to moderate Mach numbers, the rigid-body rotation is close to the one defined by the driving. As the Mach number is increased, leading to a strengthened density variation, the magnitude of the rigid-body rotation is greatly reduced and the gas becomes increasingly cooled in the geostrophic zone. This cooling counteracts the effects on the Ekman-layer

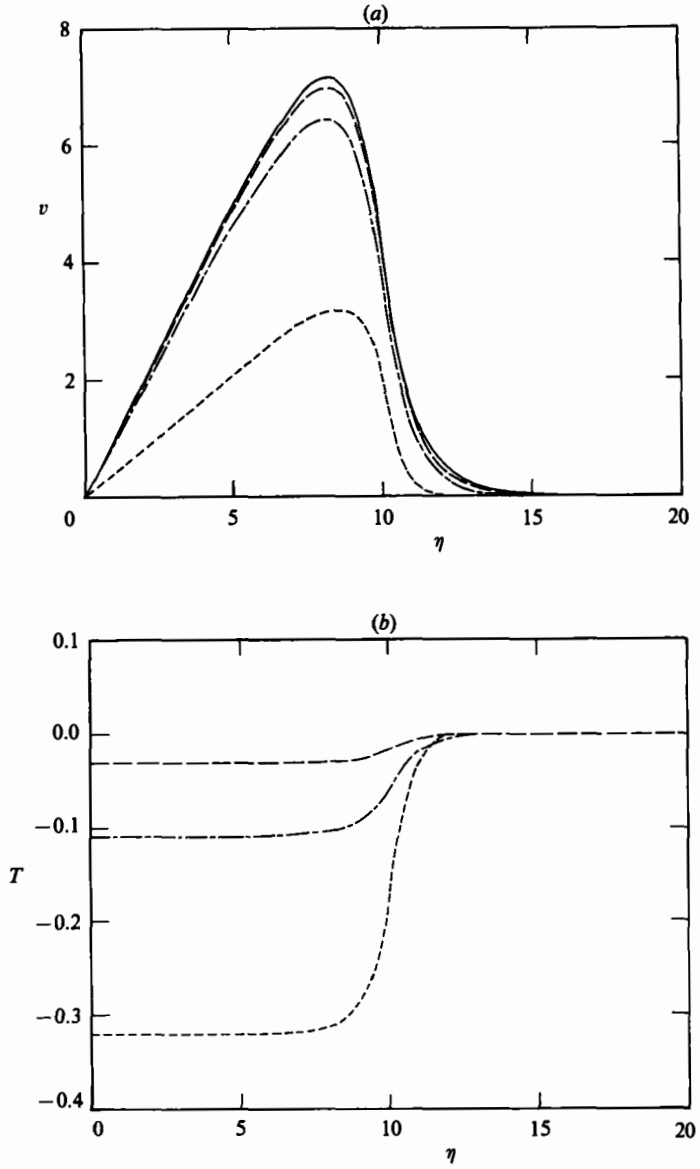

FIGURE 5. As figure 4 except $\eta_0 = 10$.

suction caused by the decrease in the rotation rate of the gas. For η_0 of $O(1)$, a geostrophic zone can no longer be clearly identified in the centre region. The swirl velocity here is one magnitude smaller than the driving and it is further reduced as the Mach number is increased. Apart from the vicinity of $\eta = \eta_0$, the temperature in the centre region is constant with the gas being cooler than the basic state. The amount of cooling does not increase monotonically with the Mach number however.

6. Conclusions

Thick $E^{\frac{1}{4}}$ Stewartson layers in a rapidly rotating gas have been investigated by numerical integration of the governing equation for layers extending in the positive radial direction and in terms of a Frobenius-series solution for layers extending in the opposite direction.

Due to the variation of the basic density field, the $E^{\frac{1}{4}}$ layer is compressed in the positive radial direction. This is in agreement with Bark & Bark (1976), whose analysis incorporated a weak density variation across the $E^{\frac{1}{4}}$ layer, and the results by Bark & Meijer (1982) for thick $E^{\frac{1}{3}}$ layers. On the other hand, $E^{\frac{1}{4}}$ layers extending in the negative radial direction are likely to extend fully to the axis of symmetry because of the density variation and, consequently, a clear distinction in terms of a geostrophic flow and an $E^{\frac{1}{4}}$-layer flow cannot always be made. Curvature effects were found to play a significant role in this case.

Appendix A: a Frobenius-series solution for the centre region

A Frobenius-series solution for the dependent variable g can be constructed in a straightforward manner. One finds

$$g = \sum_{n=0}^{+\infty} b_n \eta^{n+1}, \tag{A 1}$$

where

$$b_0 = \text{arbitrary}, \quad b_1 = \tfrac{1}{5}F_0, \tag{A 2a, b}$$

$$b_n = \frac{1}{n(n+4)}\left\{e^{-\frac{1}{4}\gamma M^2}\sum_{k=0}^{n-2} b_k d_{n-k} + (\beta - (n-\tfrac{1}{2})\kappa^2)(n+2)\, b_{n-2} + g_n \beta\kappa^2 n b_{n-4} + F_{n-1}\right\}$$

$$\text{for } n \geqslant 2, \tag{A 2c}$$

$$d_n = 0 \quad \text{for } n \text{ odd}, \tag{A 2d}$$

$$d_n = \sum_{k=0}^{\frac{1}{2}n} \frac{1}{k!}\left(\frac{\beta}{2}\right)^k e_{\frac{1}{2}n-k} \quad \text{for } n \text{ even}, \tag{A 2e}$$

$$e_0 = 1, \quad e_1 = \tfrac{5}{4}\kappa^2, \quad e_2 = \tfrac{1}{8}\kappa^4, \tag{A 2f, g, h}$$

$$e_k = \frac{(-1)^{k+1}}{k!}(\tfrac{9}{4} - k)\,\kappa^{2k} \quad \text{for } k \geqslant 3. \tag{A 2i}$$

The F_n are defined by the following series:

$$\sum_{n=0}^{+\infty} F_n \eta^n = -\rho_0^{\frac{1}{2}}(1+\kappa^2\eta^2)^{\frac{1}{4}}\frac{\mathrm{d}}{\mathrm{d}\eta}\left(\frac{1}{\eta}(v_B - \tfrac{1}{2}\eta T_B)\right), \tag{A 3}$$

$\beta = \gamma M^2/(2\eta_0^2)$ and $g_n = 0$ for $n < 4$ and $g_n = 1$ for $n \geqslant 4$. Note that if the right-hand side of (2.25a) is equal to zero, all F_n are equal to zero and only even b_n will be non-zero. The series (A 1) cannot be expected to converge in the whole interval $0 \leqslant \eta \leqslant \eta_0$ unless

$$\sigma(\gamma - 1)\, M^2 < 4. \tag{A 4}$$

Combination of the solution (A 1) with (2.21) and (2.25b, c) gives

$$v = a_0\eta + \sum_{n=0}^{+\infty} \frac{b_n}{n+2}\eta^{n+3}, \tag{A 5}$$

$$T = T_0 - 2\kappa^2 \sum_{n=0}^{+\infty} \frac{b_n}{n+4}\eta^{n+4}, \tag{A 6}$$

where T_0 is a constant and the a_0 term is the homogeneous solution used in the reduction of order. Note that, at this point, there are three arbitrary constants: a_0, b_0 and T_0. By now making use of (2.22a), (2.24), (A 1), (A 5) and (A 6), it follows that

$$b_0 = \tfrac{1}{4}e^{-\frac{1}{4}\gamma M^2}(a_0 - \tfrac{1}{2}T_0 - \omega + \tfrac{1}{2}\theta), \tag{A 7}$$

where

$$\omega = \lim_{\eta\to 0}\frac{v_B}{\eta}, \quad \theta = \lim_{\eta\to 0} T_B. \tag{A 8a, b}$$

Thus, there are two constants of integration: a_0 and T_0. This is consistent with the fact that the dependent variables in the centre region describe both the geostrophic flow and the Stewartson layer. Note that for large values of the Mach number, b_0 becomes exponentially small and the swirl velocity can be expected to approach rigid-body rotation in most of the region in the case when the series in (A 3) is identical to zero.

It turns out to be advantageous to write the solutions (A 5) and (A 6) in the form given in (3.2) and (3.3). In those equations, v_P and T_P is the particular solution obtained by letting $a_0 = b_0 = T_0 = 0$ in (A 5) and (A 6), and v_C and T_C is the homogeneous solution corresponding to the choice of $a_0 = 1$ and $b_0 = \frac{1}{4}e^{-\frac{1}{4}\gamma M^2}$ (and, of course, all $F_n = 0$).

Appendix B: the heavy-gas approximation

The case of a heavy gas is from a practical point of view an important asymptotic limit. In this case $\gamma - 1 = o(1)$ is the natural expansion parameter. For UF_6 at room temperature, this parameter equals 0.067. The leading-order problem can be obtained by equating κ^2 to zero in (2.25) and (2.21). In this limit, these equations can be integrated once. One finds

$$\frac{d^2v}{d\eta^2} + \frac{1}{\eta}\frac{dv}{d\eta} - \left(\rho_0^{\frac{1}{2}} + \frac{1}{\eta^2}\right)v = -\rho_0^{\frac{1}{2}}(c_1\eta\ln\eta + c_2\eta + v_B - \tfrac{1}{2}\eta T_B), \tag{B 1}$$

$$T = 2(c_1\ln\eta + c_2), \tag{B 2}$$

where c_2 is a constant of integration. The constants c_1 and c_2 will each take on different values in the centre and outer regions. The solution (B 2) is clearly of geostrophic nature. In what follows, it is assumed that the driving is given by (5.1) and that the slender-centrifuge approximation is valid.

In the centre region, the solutions (B 1) and (B 2) become

$$v(\eta) = (\omega + \tfrac{1}{2}T_0)\eta + Bv_C(\eta), \tag{B 3}$$

$$T = T_0 = \text{constant}, \tag{B 4}$$

where

$$v_C = \sum_{n=0}^{+\infty} a_n \eta^{2n+1}, \tag{B 5a}$$

$$a_0 = 1, \tag{B 5b}$$

$$a_n = \frac{e^{-\frac{1}{4}M^2}}{(2n+1)^2 - 1}\sum_{k=0}^{n-1}\frac{1}{k!}\left(\frac{M}{2\eta_0}\right)^{2k} a_{n-k-1}. \tag{B 5c}$$

In the outer region the following approximations to the solution of (B 1) as $\eta \to +\infty$ can be constructed:

$$v_I \approx c_1\eta\ln\frac{\eta}{\eta_p}, \tag{B 6a}$$

$$v_\pm \approx \eta^{-\frac{1}{2}}\rho_0^{-\frac{1}{8}}e^{\mp\eta_+}, \tag{B 6b}$$

where now
$$\eta_+ = \int_{\eta_0}^{\eta} \rho_0^{\frac{1}{4}}(\eta')\,\mathrm{d}\eta'. \tag{B 6c}$$

The temperature field is given by
$$T_{\mathrm{I}} = 2c_1 \ln\frac{\eta}{\eta_{\mathrm{p}}}, \tag{B 7}$$

which is an exact solution of (B 2) in the outer region.

The WKB-type solution v_+ in (B 6*b*) was used to provide starting values for a numerical integration of (B 1) using a scheme similar to the one described in §4. The approximate solution so obtained and the series solution (B 5), both valid for heavy gases, were used in testing the numerical codes for the general case.

By considering the conditions on the temperature field at $\eta = \eta_0$, namely that it and its derivative both be continuous, it follows that
$$T_0 = c_1 = 0. \tag{B 8}$$

The solution in the outer region is, hence, given by
$$v(\eta) = Cv_{\mathrm{S}}(\eta), \tag{B 9}$$

where $v_{\mathrm{S}}(\eta) \equiv v_+(\eta)$. By requiring that the azimuthal velocity and its derivative be continuous at $\eta = \eta_0$, one finds that
$$B = \frac{\omega}{W}(v_{\mathrm{S}}(\eta_0) - \eta_0 v_{\mathrm{S}}'(\eta_0)), \tag{B 10a}$$

$$C = \frac{\omega}{W}(v_{\mathrm{C}}(\eta_0) - \eta_0 v_{\mathrm{C}}'(\eta_0)), \tag{B 10b}$$

where
$$W = v_{\mathrm{C}}(\eta_0)\, v_{\mathrm{S}}'(\eta_0) - v_{\mathrm{C}}'(\eta_0)\, v_{\mathrm{S}}(\eta_0). \tag{B 10c}$$

Another interesting asymptotic limit is the small-Mach-number approximation. In this limit, the leading-order equations are given by (B 1) and (B 2) with ρ_0 replaced by unity. Hence
$$v_{\mathrm{C}}(\eta) = I_1(\eta), \tag{B 11a}$$

$$v_{\mathrm{S}}(\eta) = K_1(\eta), \tag{B 11b}$$

where I_1 and K_1 are the modified Bessel functions. The results (B 3), (B 4) and (B 7)–(B 10) also hold in this limit. It follows that
$$B = -\omega\eta_0^2 K_2(\eta_0), \tag{B 12a}$$

$$C = \omega\eta_0^2 I_2(\eta_0). \tag{B 12b}$$

It is easily verified that the homogeneous-fluid case is recovered by letting $\eta_0 \to +\infty$ in the results (B 3), (B 8), (B 9), (B 11) and (B 12).

REFERENCES

Bark, F. H. & Bark, T. H. 1976 On vertical boundary layers in a rapidly rotating gas. *J. Fluid Mech.* **78**, 749.

Bark, F. H. & Bark, T. H. 1979 On axially antisymmetric geostrophic flows in rapidly rotating gases. *J. Méc.* **18**, 47.

Bark, F. H. & Hultgren, L. S. 1979 On the effects of thermally insulating boundaries on geostrophic flows in rapidly rotating gases. *J. Fluid Mech.* **95**, 97.

BARK, F. H. & MEIJER, P. S. 1982 Effects of circumferential curvature and radial stratification on Stewartson $E^{\frac{1}{4}}$ layers in a rapidly rotating gas. *FFA Tech. Note* 1982-44.

COLLATZ, L. 1960 *The Numerical Treatment of Differential Equations*, 3rd edn. Springer.

DURIVAULT, J. & LOUVET, P. 1976 Etude de la couche de Stewartson compressible dans une centrifugeuse à contre-courant thermique. *C. R. Acad. Sci. Paris* **283** (B), 79.

DURIVAULT, J., LOUVET, P., ROUVILLOS, G. & SOUBBARAMAYER, X. 1976 Thermal counter current and isotope separation in a centrifuge with an isothermal side wall. *C. R. Acad. Sci. Paris* **283** (B), 17.

HASHIMOTO, K. 1977 Flows in a rapidly rotating cylinder. Ph.D. thesis, Kyoto University, Japan.

HOWARD, L. N. 1970 Rotating and stratified flows. In *Mathematical Problems in the Geophysical Sciences*. Lectures in Applied Mathematics, vol. 13, p. 121. American Mathematics Society.

HULTGREN, L. S., MEIJER, P. S. & BARK, F. H. 1981 On axisymmetric time-dependent source flows in a rapidly rotating gas. *J. Méc.* **20**, 135.

LOUVET, P. & DURIVAULT, J. 1976 Paper presented at the Symposium on Singular Perturbation Problems and Boundary-layer Theory, Lyon, France.

MIKAMI, H. 1973 Thermally induced flow in gas centrifuge. *J. Nucl. Sci. Tech.* **10**, 580.

NAKAYAMA, H. M. & USUI, S. 1974 Flow in a rotating cylinder of a gas centrifuge. *J. Nucl. Sci. Tech.* **11**, 242.

OLANDER, D. R. 1978 The gas centrifuge. *Sci. Am.* **239** (2), 27.

SAKURAI, T. & MATSUDA, T. 1974 Gasdynamics of a centrifugal machine. *J. Fluid Mech.* **62**, 727.

WOOD, H. G., JORDAN, J. A. & GUNZBURGER, M. D. 1984 The effects of curvature on the flow field in rapidly rotating gas centrifuges. *J. Fluid Mech.* **140**, 373.

WOOD, H. G. & MORTON, J. B. 1980 Onsager's pancake approximation for the fluid dynamics of a gas centrifuge. *J. Fluid Mech.* **101**, 1.